Journal of
Computational and Theoretical Nanoscience
Vol. 4, 1–6, 2007

Study of Solid–Liquid Phase Changes of Lennard-Jones Nanoclusters by NPT Monte Carlo Simulations

Silvina M. Gatica[1, 2, *], Xiao Dong[2], and Estela Blaisten-Barojas[2]

[1] *Department of Physics and Astronomy, Howard University, Washington, DC 20059, USA*
[2] *Computational Materials Science Center, George Mason University, Fairfax, VA 22030, USA*

NPT Monte Carlo classical computer simulations were performed to study the structure and thermal equilibrium properties of Lennard-Jones clusters. Three sizes were considered in the study, with 38, 42, and 50 atoms, temperatures from 0.1 to 0.5 and pressures from 0 to 20 (in reduced units). For the three clusters we observe a discontinuity in the slope of the isotherms that corresponds to a rearrangement of the atoms in shells inside the cluster. For the cluster of 50 atoms we found a peak in the specific heat at a temperature $T = 0.26$ and pressure $P = 1$. This finding is consistent with the predictions of other authors. According to the characteristics of the radial distribution function, this peak is related to a liquid–solid phase change.

Keywords: Clusters, Lennard-Jones, Phase-Transitions.

RESEARCH ARTICLE

1. INTRODUCTION

The investigation of properties of small clusters is a subject of great theoretical and experimental interest.[1–12] The recent developments in nanotechnology gave new incentive to the study of clusters with diameters in the nanometer range (nanoclusters). The properties of such nanoclusters are very different than the properties of the bulk because of the large surface/volume ratio in the clusters. Numerous studies were carried out to predict the melting temperature and mechanisms of clusters. For example, Franz[3] performed Monte Carlo (MC) calculations for confined Argon clusters with 25 to 60 atoms finding that the specific heat has one or two peaks at different temperatures, one of which may be associated with solid–liquid phase-changes. Ding et al.[4] performed Molecular Dynamics (MD) studies of free and supported iron clusters finding estimations of the melting temperatures based on the Lindemann criterion. Studies with many-body potentials and MD for the alkali metal nanoclusters also reported melting temperatures based on the Lindemann criterion.[5] Recent MD tight-binding approaches to describe the dynamics of calcium nanoclusters, also used this criterion for estimates of melting temperatures.[6]

The focus of this work concerns studies where the interactions that keep a cluster together are the van der Waals forces between atoms. For rare gases this force is well represented by the pair-wise additive Lennard-Jones potential (LJ) given by

$$U_{\mathrm{LJ}}(r) = 4\varepsilon\left\{(\sigma/r)^{12} - (\sigma/r)^{6}\right\} \tag{1}$$

where σ and ε are parameters of the potential and r is the interatomic distance. Computer simulations have served for extensive studies of bulk LJ systems and the phase diagram has been determined.[13] On the other hand, size dependent phase diagrams of nanoclusters are still lacking, even for simple models such as the LJ. Studies of systems interacting via the LJ potential usually employ reduced units (units of energy, length, and pressure equal to ε, σ, and ε/σ^3, respectively). In the rest of this article we will use this set of units. For example, for bulk LJ the melting temperature (T_{m}) is 0.68 at $P = 0.01$ and at higher pressures T_{m} increases linearly with P.

At high temperature and low pressure clusters tend to disaggregate by evaporation. To prevent this phenomenon and make possible the computation of equilibrium properties, in most MC simulations the cluster is confined into a rigid box and consequently the results depend strongly on the size of the box.[3, 7, 8, 12] In this work we study free clusters, i.e., without confinement, using the isothermal isobaric Monte Carlo (NPT-MC) method. The NPT-MC is commonly used to study systems in the vicinity of phase transitions and to simulate a situation that resembles the conditions of the experiment, which are fixed external T

*Author to whom correspondence should be addressed.

and P. In our simulations T and P are input parameters, while the volume $V(T, P)$ and the energy $E(T, P)$ are outcomes of the calculation. Based on these T, P dependent properties we compute the specific heat and other thermodynamic properties.

This article is organized as follows. In Section 2 we discuss the thermodynamic properties of the clusters, in Section 3 we focus on the structure and in the last section we present our conclusions.

2. THERMODYNAMIC PROPERTIES OF LJ CLUSTERS FROM NPT MC CALCULATIONS

In the NPT Monte Carlo the volume of the system fluctuates to ensure the condition of constant pressure. In each MC step, the possible moves include the expansion or compression of the system that is done randomly in the same way the atoms are shifted. [14]In our calculations we did approximately 4×10^6 MC moves and the ratio between volume moves to atoms shifts was fixed at 10%. The MC step was dynamically adjusted to keep an acceptance rate of about 50% along the runs.

The volume of the cluster was computed in terms of the root-mean-square radius $R = \langle r^2 \rangle^{1/2}$ as $V = 4/3\pi(5/3)^{3/2}R^3$, where r is the position of each atom with respect to the center of mass. This last equation is exact for the case of a uniform sphere. The number densities $\rho = N/V$ obtained with this formula for the global minimum configurations (g.m) of LJ_{38}, LJ_{43}, and LJ_{50} are 1.126, 1.06, and 1.09, respectively. The g.m is the structure with lowest potential energy at zero temperature, and can be found in the Cambridge Cluster Database.[15] In Figure 1 we display the g.m. for $N = 38$, 43, and 50. The energy

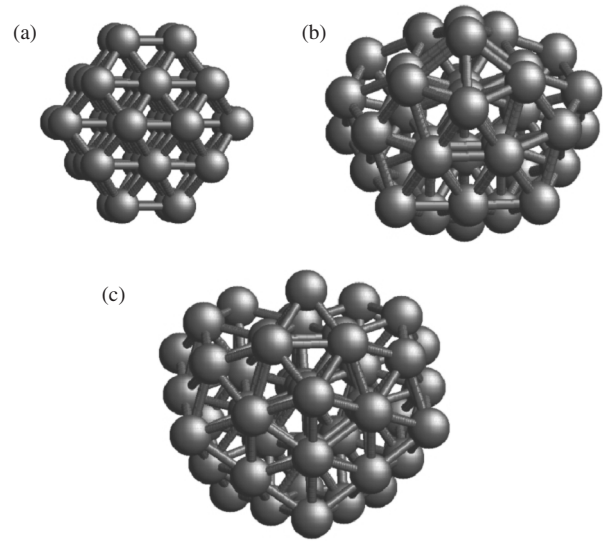

Fig. 1. Global-minimum configurations for LJ clusters with (a) 38, (b) 43, and (c) 50 atoms.

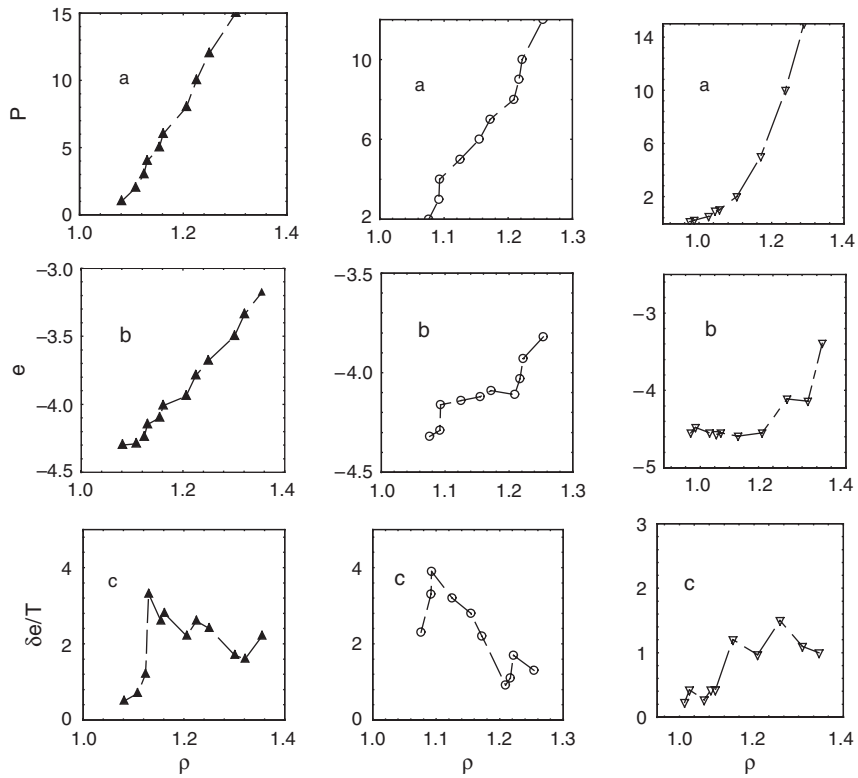

Fig. 2. Pressure (a), energy per particle (b), and energy per particle fluctuations (c) as functions of ρ for clusters LJ_{38} (left column), LJ_{43} (center column), and LJ_{50} (right column) along the $T = 0.1$ isotherm.

per particle of the g.m.'s are −4.58, −4.706, and −4.89 for $N = 38$, 43, and 50, respectively.

The equilibrium properties of the clusters at different pressures along various isotherms were studied first. The initial configuration is set in a cubic lattice with lattice constant equal to one. If a solid–liquid-like phase change takes place at a given pressure, there would be signatures like discontinuities in the slope of the PV isotherms as well as the energy per particle. Plots in Figure 2(a) depict the PV isotherm at $T = 0.1$ for the clusters LJ_{38}(left), LJ_{43} (center), and LJ_{50} (right). We see that for this cluster there is an abrupt change in the slope of $P(V)$ at $\rho = 1.093$ (central plot in Fig. 2(a)).

The fluctuations of the energy per particle were also examined,

$$\delta e = (\langle e^2 \rangle - \langle e \rangle^2)^{1/2} \tag{2}$$

where $\langle e \rangle = \langle \text{total potential energy} \rangle / N$. In the regions of phase transitions the fluctuations are usually enhanced. In Figures 2(b) and 2(c), the average energies and their fluctuations are shown for the three cluster sizes (38, 43, 50) at the same temperature of $T = 0.1$. It is visible that for the LJ_{43} (Figs. 2(b), (c) center) the discontinuity in the slope of the PV isotherm is accompanied by a step up in the energy per particle and a peak in the energy fluctuations. A less pronounced, similar pattern is observed in the cluster LJ_{38} at $\rho = 1.125$.

For the 50-atom cluster, as shown in Figure 2 to the right, the PV isotherm PV is smooth and there are no significant features in the energy per particle or energy fluctuations at this low temperature. However for this cluster size, the discontinuous slope in PV isotherms reappears at higher temperatures, as seen in Figure 3 for the isotherms $T = 0.2$ to 0.4 where the kink is apparent at densities 1.14, 1.03, and 1.12 for $T = 0.2$, 0.3, and 0.4, respectively. The effect is more evident for the higher temperatures.

For the case $N = 50$, other thermal properties were also studied, such as the temperature dependence of the equilibrium properties at a fixed pressure. Figure 4 illustrate results of the energy per particle and the cluster density as a function of the temperature for $P = 1$ and 10. For $P = 10$ the curves are monotonic, while for $P = 1$ there is a jump at $T = 0.26$. Additionally, the specific heat per particle at constant pressure, C_P, was calculated from

$$C_P/k_B = 3/2 + (\partial e/\partial T)_P - (P/\rho^2)(\partial \rho/\partial T)_P \tag{3}$$

where the first term accounts for the kinetic energy contribution per particle, which is not included in e. The results

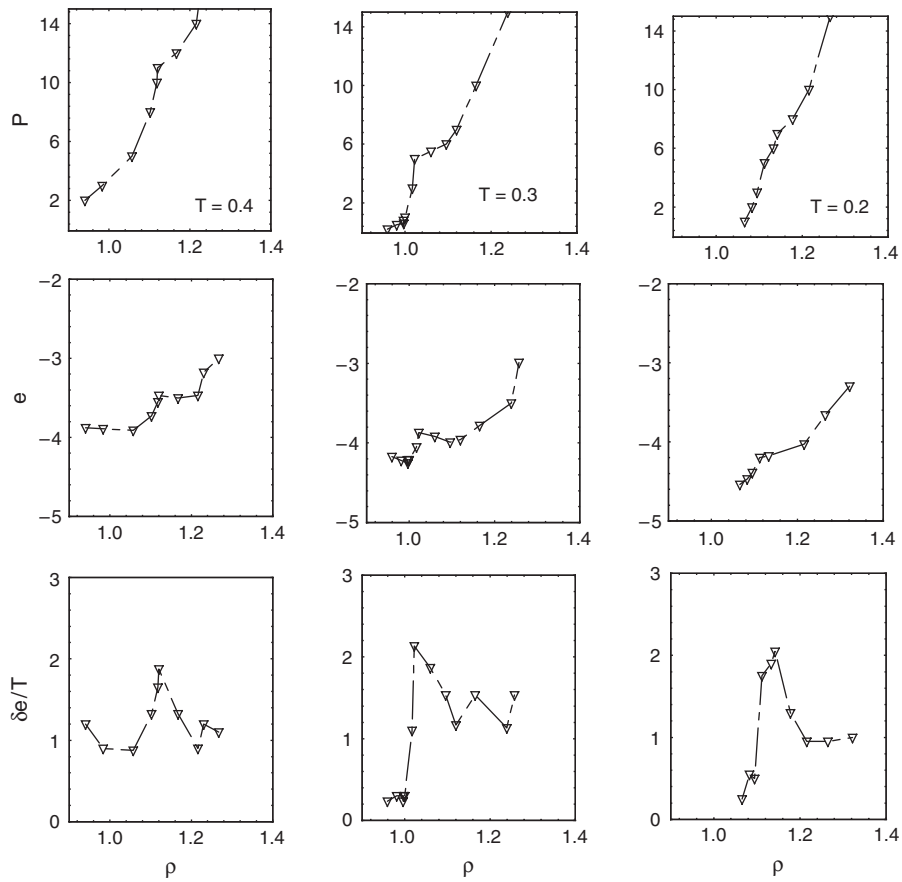

Fig. 3. For a cluster LJ_{50}, pressure (top), energy per particle (center), and energy per particle fluctuations (bottom) as function of ρ along the isotherms $T = 0.2$, 0.3, and 0.4 from right to left.

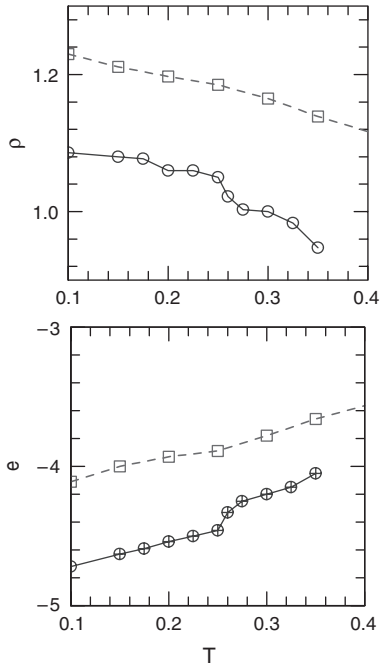

Fig. 4. For the $N = 50$ cluster, energy per and particle (bottom) and density (top) as a function of temperature at $P = 1$ (solid line) and $P = 10$ (dashed line).

are presented in Figure 5. For $P = 1$ we see a peak associated to the step in the energy and density shown in Figure 4, at $T^* = 0.26$. No peak is present at $P = 10$.

Franz[3] reports a peak in the C_V at a similar temperature (0.25) for Ar_{50}. Similar results are reported by Frantsuzov et al. though at a slightly lower temperature. Both authors relate the peaks to a melting process. In order to explore this possibility, in the next section we look at the structure of the cluster around at temperatures around T^*.

3. EFFECTS OF THE PRESSURE AND TEMPERATURE ON THE STRUCTURE OF THE LJ CLUSTERS

Static structural changes were studied with radial distribution function (RDF) $g(r)$ defined as

$$g(r) = V/N^2\langle\Sigma_i\Sigma_{j>i}\delta(r - r_{ij})\rangle \qquad (4)$$

The results are displayed in Figure 6 for the cluster LJ_{50} at temperatures $T = 0.0$, 0.2, and 0.3. At $T = 0.0$ the RDF reflects the structure of the global minimum, with a characteristic main peak at $r = 1.1$ followed by well-defined secondary peaks. This structure is not lost at $T = 0.2$, yet disappears at $T = 0.3$ where the function $g(r)$ has the aspect of a liquid-like phase with a double-hump second peak and a third peak at $r = 2.8$. There is clearly a qualitative change in the RDF as the temperature increases above $T^* = 0.26$. This supports the conclusion that the peak in the specific heat C_P is associated to a solid–liquid phase change.

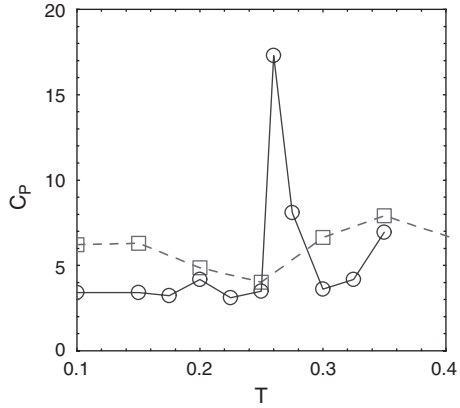

Fig. 5. Specific heat C_P per particle as a function of the temperature for $P = 1$ (solid line) and $P = 10$ (dashed line), $N = 50$.

Returning to the question of correlating the sudden change of slope of the curves $P(V)$ seen in Figures 2 and 3 with melting, comparison was made among the RDF's above and below the pressure at which the kink

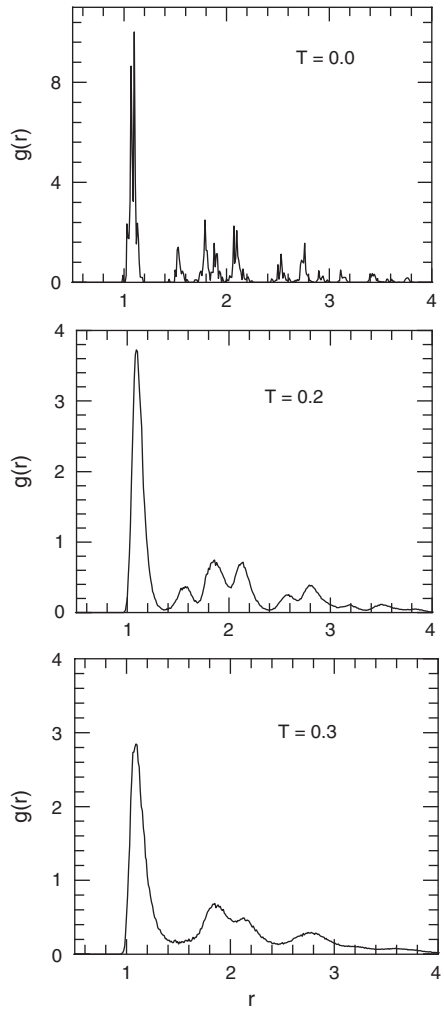

Fig. 6. Radial distribution function for the cluster LJ_{50} at $P = 1$ and temperatures indicated in the legend.

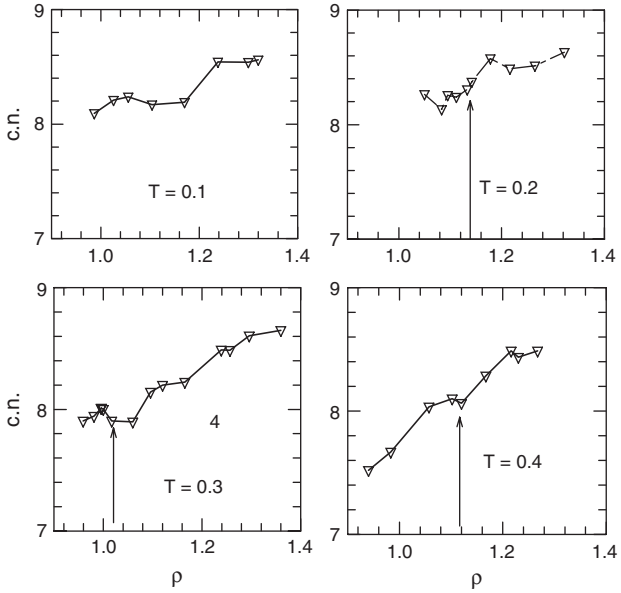

Fig. 7. Coordination number as a function of the density for LJ_{50} along the isotherms $T = 0.1$, 0.2, 0.3, and 0.4. The arrow indicates the value of ρ^*.

was observed. For the cluster LJ_{50} (Fig. 3), the kink is approximately at $P = 6$ for the isotherm $T = 0.2$. However, comparison of the RDF at $P = 5$ and $P = 8$ showed no qualitative difference, both of them looking as liquid-phase-like shown in the bottom row of Figure 6.

In order to understand the structural change associated to this feature in the isotherms we calculated the coordination number (c.n.), which is defined as the average number of nearest neighbors for each atom in the cluster. In bulk LJ systems, the c.n. is smaller for liquids taking values between 8 and 9 than for solids where c.n. is 12 for the fcc lattice. In clusters the c.n. has lower values than in bulk due to the effect of the surface. The c.n. can be calculated as the 3D integration of the first peak of the RDF up to the value of r consistent with the first coordination shell (or first-neighbor distance). For the LJ clusters with $N = 38$, 43, and 50 in the structure corresponding to their g.m., the c.n. is 6.38, 7.43, and 7.09, respectively. In Figure 7 we show the c.n. as a function of the density for the cluster LJ_{50} at temperatures from 0.1 to 0.4. We marked with an arrow the position of the kinks in the isotherms $P(V)$

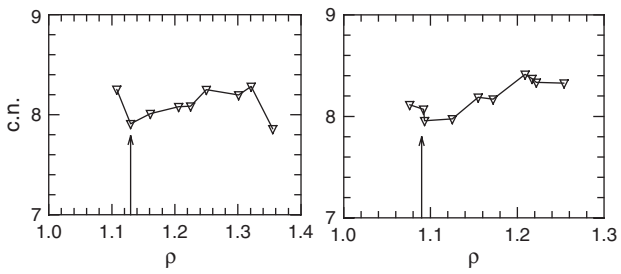

Fig. 8. Coordination number as a function of the density for LJ_{38} (left) and LJ_{43} (right) at $T = 0.1$. Arrows indicate the value of ρ^*.

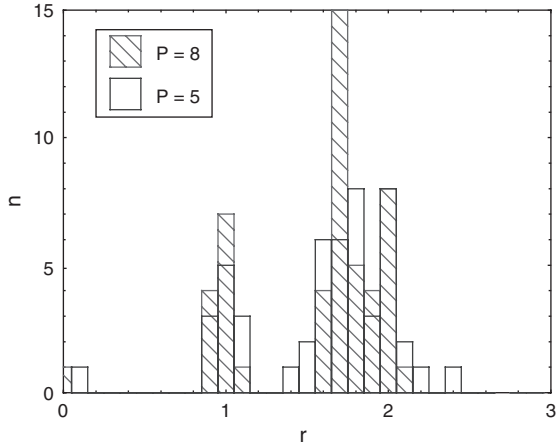

Fig. 9. Number of particles as a function of the distance to the center of mass of the cluster for $N = 50$ and $T = 0.2$. The pressure is $P = 5$ (solid boxes) and $P = 8$ (dashed boxes).

(Fig. 3). We see that, as the density increases in the vicinity of the kink, the c.n. steps down for $T = 0.3$ and 0.4 and increases smoothly for $T = 0.1$ and 0.2. Similar results were obtained for the LJ_{38} and LJ_{43} clusters, as seen in Figure 8. Thus there is no signature in the c.n. that could be linked to the discontinuous slope in the curve $P(V)$ and sudden increase in the energy.

Finally, we did a simple analysis of the configurations that gives insight of the process involved at ρ^*. In order to do a quantitative analysis of the structure of the clusters we plotted histograms showing the number of atoms as a function of the distance from the center of mass. Each bin in the histogram would be associated to a spherical shell centered at the center of mass. The results are displayed in Figure 9 for $N = 50$ at $T = 0.2$ and pressures 5 and 8. We see in this figure that for both pressures most of the atoms are confined into two distinguishable shells. At the lower pressure the outer shell spreads outwards. At the higher pressure there is a high concentration of atoms at a distance $r = 1.7$. The situation remains the same for all cluster configurations inspected at high or low P. Thus, the sudden increase in the energy when crossing ρ^* reflects the compression of the outer shell.

4. CONCLUSIONS

We have applied the method of Monte Carlo at constant temperature and pressure to the study of small free clusters. We have investigated the structural and thermal equilibrium properties of LJ clusters with 38, 43, and 50 atoms at low temperatures and high pressures. For the cluster with 50 atoms at $P = 1$ we found a peak in the specific heat at constant pressure at a temperature of 0.26 that suggests a solid–liquid phase change. This is supported by a qualitative change in the RDF as the temperature decreases below 0.26 at $P = 1$. For $P > 1$ the peak in C_P was not encountered, suggesting the possibility of the transition

being suppressed at higher pressures. To be conclusive about this conjecture, higher temperatures should be investigated as will be addressed in future work.

Extending the calculations presented in this work it is possible to systematically construct the melting curve of free clusters at finite pressures. Since the calculation is done without confining the cluster in a cell, the results do not depend on any additional external parameters such as the size of the box.

References

1. M. Barranco, R. Guardiola, S. Hernandez R. Mayol, J. Navarro, and M. Pi, *J. Low Temp. Phys.* 142, 1 **(2006)**.
2. X. Dong and E. Blaisten-Barojas, *J. Comput. Theor. Nanosci.* 3, 118 **(2006)**.
3. D. D. Frantz, *J. Chem. Phys.* 115, 6136 **(2001)**; R. S. Berry and B. M. Smirnov, *J. Non-crystalline Solids* 351, 1543 **(2005)**.
4. F. Ding, A. Rosen, S. Curtarolo, and K. Bolton, *Appl. Phys. Lett.* 88, 133110 **(2006)**.
5. Y. Li, E. Blaisten-Barojas, and D. A. Papaconstantopoulos, *Phys. Rev. B* 57, 15519 **(1998)**.
6. X. Dong, G. M. Wang, and E. Blaisten-Barojas, *Phys. Rev. B* 70, 205409 **(2004)**.
7. J. P. Neirotti, F. Calvo, D. L. Freeman, and J. D. Doll, *J. Chem. Phys.* 112, 10340 **(2000)**.
8. D. Sabo, D. L. Freeman, and J. D. Doll, *J. Chem. Phys.* 122, 094716 **(2005)**.
9. Ph. Buffat and J.-P. Borel, *Phys. Rev. A* 13, 2287 **(1976)**.
10. S. L. Lai, J. Y. Guo, V. Petrova, G. Ramanath, and L. H. Allen, *Phys. Rev. Lett.* 77, 99 **(1996)**.
11. M. Dippel, A. Maier, V. Gimple, H. Wider, W. E. Evenson, R. L. Rasera, and G. Schatz, *Phys. Rev. Lett.* 87, 095505 **(2001)**.
12. P. A. Frantsuzov and V. A. Mandelshtam, *Phys. Rev. E* 72, 037102 **(2005)**.
13. A. Jackson, Structural Phase Behavior Via Monte Carlo Techniques, Thesis doctorate University of Edinburg, UK **(2001)**.
14. D. Frenkel and B. Smit, Understanding Molecular Simulation, Computational Science Series Vol. II, Academic Press, New York **(2002)**.
15. http://www-wales.ch.cam.ac.uk/CCD.html

Received: 24 August 2006. Accepted: 9 September 2006.